

# Application of Material Characterization to Research & Development of Polypropylenes

Sumitomo Chemical Co., Ltd.

Petrochemicals Research Laboratory

Takashi SAKURAI

Shizuto YAMAKOSHI

Kenji WATANABE

Naoya UMEGAKI

Value-added polypropylene is one of the industrial materials desirable for saving energy and reducing stress on environment. As the material performance becomes multi-functional and advanced, material characterization plays an important role because of the complicated material characteristics. The speedy application of suitable characterization methods is very effective for promoting the research and development activities. In this article, we introduce some examples of the application to evaluate polypropylene film and compound.

This paper is translated from R&D Report, “SUMITOMO KAGAKU”, vol. 2012.

## Introduction

Polypropylene is currently used in various industrial products such as food packaging, consumer electronics and parts of automobiles, making the most of its special features such as light weight, high rigidity and high cost performance. In recent years new value-added polypropylene has been produced, contributing to the realization of energy conservation and low environmental impact. Research and development aiming to achieve higher performance by adding new functionalities and making lighter-weight products through the improvement of mechanical performance are now actively being conducted. From this point forward, demand for polypropylene is expected to grow in many more industries, and thus control technologies for catalysts and polymerization processing, as well as more advanced compound and molding technologies, will be needed.

As high-value-added materials have become increasingly popular, the importance of basic analytical technologies such as structural analysis and simulation in research and development activities has increased more than ever. Crystalline polymers such as polypropylene form a hierarchical structure in a wide scale from sub-nanometers to micrometers. As various kinds of structures (such as the crystals and amorphous structures and the interface structure of compounds observed at the nano scale, and the spherulite structure and phase structure of compounds observed at the micron scale)

have become increasingly complex, data analyses and interpretations have also become more complex. Furthermore, in order to discuss the correlations between structure and its physical properties, it often requires an advanced structural analysis technology through which one can observe how the structure changes in the process of deformation and crystallization of the material in real time.

Given such circumstances, we at Sumitomo Chemical Co., Ltd. are proactively promoting basic analytical technology by brushing up the existing analysis technology and collaboration with external research institutions, in order to more rapidly and efficiently lead the outcomes of our research and development in business.

This paper introduces the application of structural analysis technology to polypropylene material development, using as examples the recent cases of its application to films and compounds.

## Structural Analysis of Films

### 1. Application to Capacitor Films

Polypropylene films are used in applications such as food packaging, industrial materials, pharmaceuticals and electronic products. In recent years, the demand for high-value-added films—including thin films for packaging, capacitor films, films for boil in the bag food and industrial protection films—has expanded in the market.

A capacitor is an apparatus that stores and releases an electric charge. In Japan, it is also commonly called a condenser. Along with the increased demand for hybrid vehicles as well as the commercialization of electric vehicles, the research and development of polypropylenes has intensified for the purpose of achieving large-capacity capacitors. **Fig. 1** shows a schematic illustration of an orbiting-type capacitor. Due to the characteristics of polypropylenes, which are characterized by high breakdown voltage and small dielectric loss, polypropylene film is used for the capacitor dielectrics.

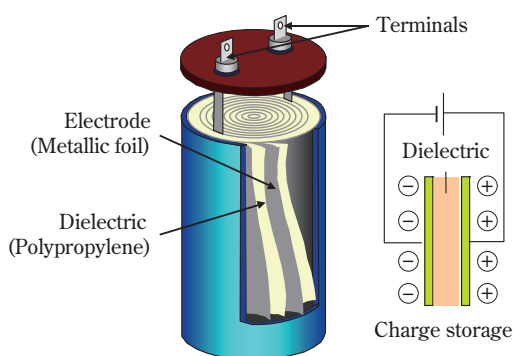


**Fig. 1** Structure of a capacitor and mechanism of charge storage

Industrially speaking, a polypropylene film for capacitors is produced through a sequential biaxial drawing process as shown in **Fig. 2**. In this process the molten resin extruded from the die is crystallized first, thus forming original undrawn film.

The next step is the MD (machine direction) drawing process, in which the original undrawn film is drawn by using several rolls, taking advantage of the differences in the speed of rotation between the rolls. In the TD (transverse direction) drawing process that is subsequently performed, a film is produced by

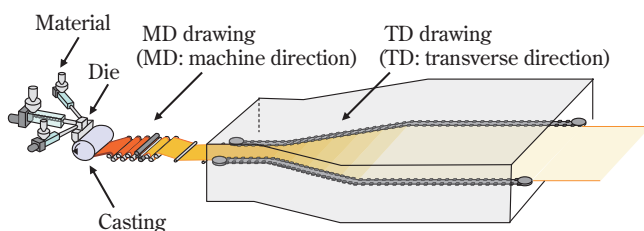


**Fig. 2** Schematic illustration of sequentially biaxial drawing process

drawing the film toward the direction perpendicular to the MD.

When producing a polypropylene film for capacitors, it is necessary to allow the film surface to have an appropriate level of roughness to add an insulating-oil impregnating ability to the film. This characteristic is one of the most significant special features of polypropylene film as compared to regular packaging films, of which the important special feature is a smooth surface. As for a roughing method, the use of crystalline polymorphism in polypropylene is the most effective selection.<sup>1)</sup>

In this method, which uses crystalline polymorphism, phenomena such as crystal transition may occur upon film production, and consequently the control of the film structure can be extremely complex. Thus structural analysis technology plays an important role when clarifying the surface roughening mechanism and constructing a control technology for rough surface configurations. This paper introduces the technique by which to observe the drawing behavior by presenting examples of its application in polypropylene for capacitors.

## 2. Special Features of Polypropylene for Capacitors

Many of the original undrawn sheets used to produce food packaging film through a sequential biaxial drawing process have a spherulite structure ( $\alpha$ -spherulite), consisting of crystals of polypropylene called  $\alpha$ -crystals. However, in some original polypropylene undrawn sheets, another spherulite structure ( $\beta$ -spherulite) composed of polypropylene crystals called  $\beta$ -crystals, which are different from  $\alpha$ -crystals, is often observed as well. **Fig. 3** shows the optical microscopic image and the X-ray diffraction pattern of polypropylene having both  $\alpha$ - and  $\beta$ -crystals. Because birefringence differs between the  $\alpha$ - and  $\beta$ -crystals, the  $\beta$ -spherulites are visible in bright light and can thus be distinguished from the  $\alpha$ -spherulites by a simple microscopic observation under orthogonal polarization.<sup>2)</sup> Moreover, because the unit lattice differs between the  $\alpha$ - and  $\beta$ -crystals, and because a diffraction peak unique to the  $\beta$ -crystals ((300) planes) can be observed, the amount of  $\beta$ -crystals can be estimated through the X-ray diffraction pattern. Although there are still scientifically unknown factors in the mechanism by which  $\beta$ -crystals form, it has already been revealed that the molding conditions of

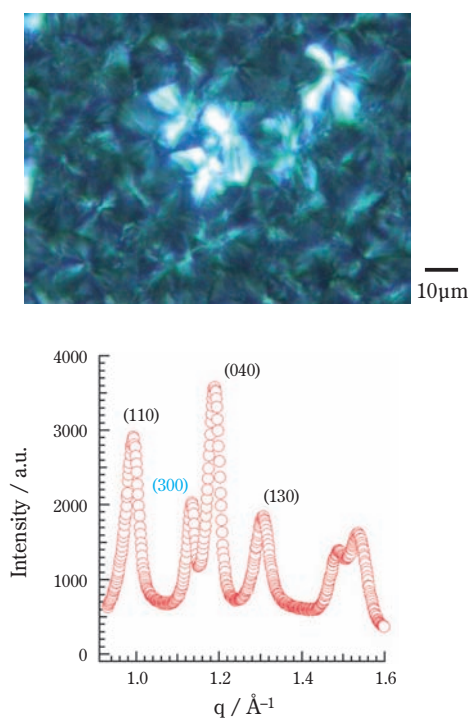


**Fig. 3** Optical image and X-ray diffraction pattern of polypropylene with polymorphs: (110), (040) and (130) is the reflection peak of  $\alpha$ -crystals and (300) is that of  $\beta$ -crystals, respectively

the original undrawn sheet and the addition of a  $\beta$ -crystal nucleating agent affect the size, amount and distribution of the  $\beta$ -spherulites.<sup>3)</sup>

### 3. Observation of the Drawing Behavior Using an Optical Microscope

By combining an optical microscope and a commercially available heat-drawing apparatus, the drawing behavior of the film can be readily observed. This

technique is referred to as TOA (Thermo Optical Analysis), and is an effective technique for films used in capacitors. **Fig. 4** shows the outline of the observation system. Our objective in this experiment was to observe the drawing behavior of the film when stretched in both the machine and transverse directions during the sequential biaxial drawing process.

**Fig. 5** shows the observed polarized optical microscope (POM) images. Upon observation, the images were enhanced by inserting a sensitive color plate in the orthogonal polarization state. For the observation of the MD drawing behavior (A) we used a film having a thickness of 20  $\mu\text{m}$ , which had been made by cutting off the surface layer of the original undrawn sheet using an ultramicrotome. For the observation of the TD drawing behavior (B), a MD drawing film (thickness of 80  $\mu\text{m}$ ), which had been manufactured by a drawing machine, was used as is. The elongation temperature was set at 140°C for both observations. During the experiment on the MD drawing behavior it was observed that the  $\beta$ -spherulite region with high luminance (figure (a)) transformed to a dark elliptical shape (figure (b)) when necking occurred, after which it stretched further (figure (c)). It can be considered that oval-shaped hollows (figure (d)) on the film which were formed in the MD drawing process were caused by the  $\beta$ -spherulites. Furthermore, in the figure of the TD drawing process one can clearly observe how the oval-shaped hollows form surface roughness on the film (figure (f)). Thus it can be assumed that the formation of surface roughness on polypropylene films for capacitors can be triggered by the  $\beta$ -spherulites and that it is created due to TD drawing after going through the oval-shaped hollow state.

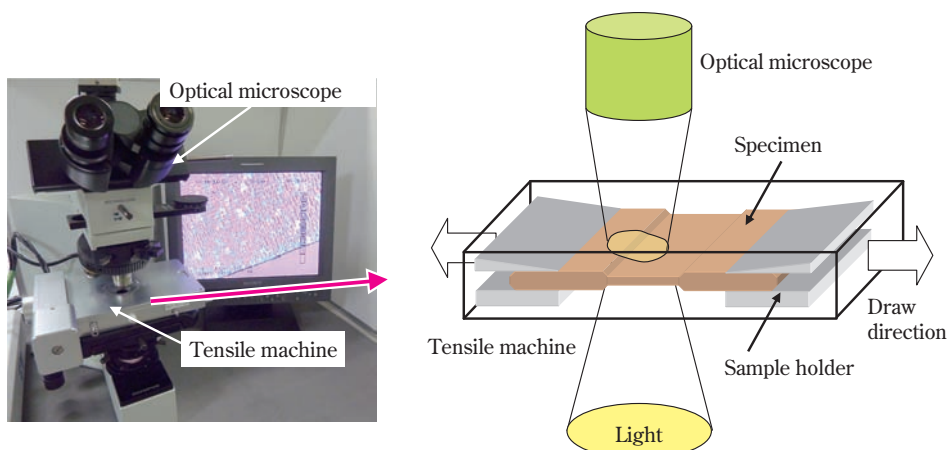


**Fig. 4** Experimental system for observing the drawing process by optical microscope

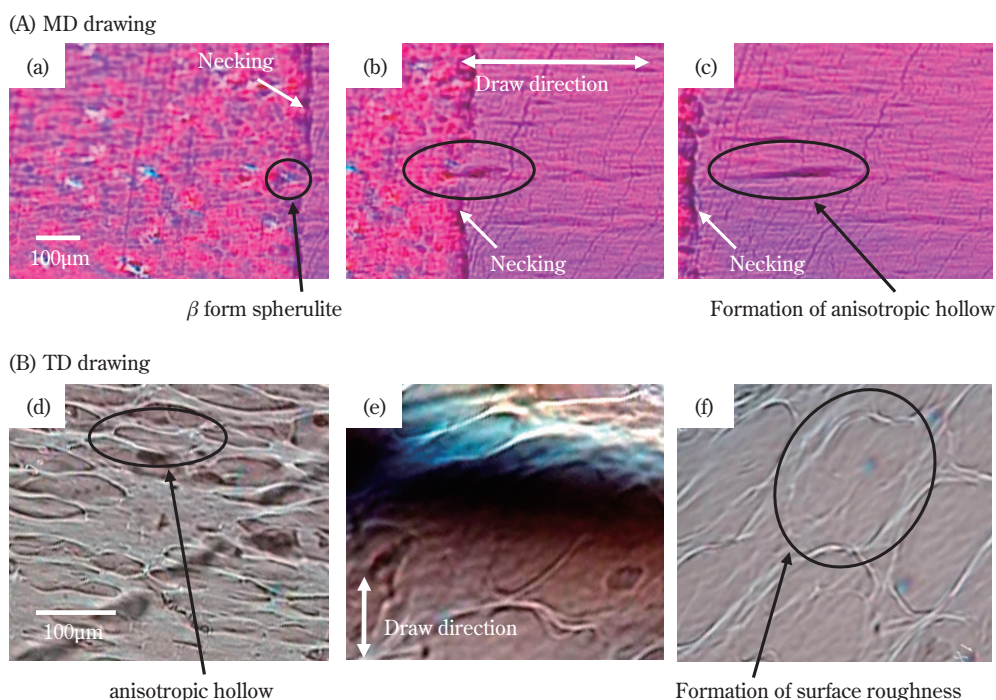


**Fig. 5** Optical images of film deformation in (A) MD and (B) TD drawing process

#### 4. Observation of the Drawing Behavior Using a Synchrotron Radiation X-ray

It has been reported that  $\beta$ -crystals of polypropylene are metastable, whereby they transform into  $\alpha$ -crystals under the appropriate thermal conditions and constant stress.<sup>3)</sup> Generally, X-ray diffraction and scattering methods are used for the structural analysis of crystals. Of those methods, diffraction and the scattering methods that use a high-performance synchrotron radiation X-ray with high brilliance are highly effective when tracing the structural change (which occurs during the drawing process) in greater detail. One reason for this is that information on the crystalline structure can be obtained by those methods in the order of milliseconds, although it normally takes several hours when using commercially grade X-ray generators. That is the time resolution adequate for tracking the transformation behavior of the crystalline structure. The second reason is that such methods make it possible to examine the local-area deformation behavior of the film using X-rays narrowed to the micron order as the radiation source. For more details about technologies using synchrotron radiation in macromolecules, refer to the various papers available.<sup>4)–10)</sup> This paper presents examples of observing the MD drawing behavior using general millimeter-scale macrobeam and microbeam X-rays which have been narrowed down to the micron order.

Initially, small- and wide-angle X-ray scattering with macrobeams as the radiation source were simultaneously measured using the beamline (BL06A) of the High Energy Accelerator Research Organization (KEK). **Fig. 6** shows the time evolution of the X-ray diffraction (WAXD) profiles obtained when the original undrawn film (with the thickness of 100  $\mu\text{m}$ ) having both  $\alpha$ - and  $\beta$ - spherulites was drawn during the MD drawing process (at a temperature of 120°C). Information about the crystalline polymorphism can be obtained from the peak WAXD pattern. Furthermore, **Fig. 7** indicates the time evolution of full width at half maximum (FWHM) of the WAXD peak. Information about the order of crystals can be obtained from the FWHM. Although the intensity of the WAXD peak of the  $\beta$ -crystals suddenly drops at around 35 sec, when necking occurs to the X-ray irradiated area of the film, no obvious change can be observed during the drawing process. In the meantime, the FWHM extends during the drawing process, thereby demonstrating that the order of the crystals is gradually disordered by the drawing.

**Fig. 8** shows the time evolution of the small-angle X-ray scattering (SAXS) profile compared with the film having  $\alpha$ - and  $\beta$ -spherulites and the original undrawn film having  $\alpha$ -spherulites alone. Prior to the drawing process, the scattering peak derived from the structural period of the crystalline and amorphous phase called



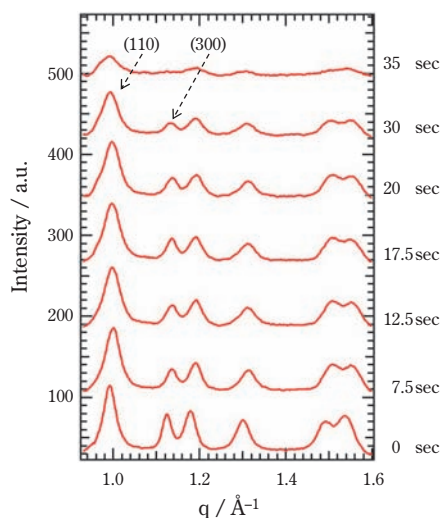


**Fig. 6** Time evolution of circular averaged WAXD profiles observed for film with  $\alpha$ - and  $\beta$ -spherulites during MD drawing

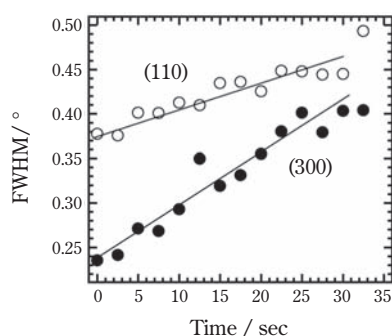


**Fig. 7** Time evolution of FWHM (Full width at half maximum) observed for film with  $\alpha$ - and  $\beta$ -spherulites during MD drawing: open and filled circles are (110) reflection of  $\alpha$ -crystal and (300) reflection of  $\beta$ -crystal, respectively

the long-period structure can be observed. The original undrawn film having both the  $\alpha$ - and  $\beta$ -spherulites demonstrates a characteristic that other than the scattering peak derived from the long-period structure, strong scattering intensity due to microvoids can be observed in the low-wavenumber region ( $q < 0.2$ ) at around 12.5 sec. Additionally, as shown in **Fig. 6** which shows the WAXD profiles, it can be guessed that plastic deformation has occurred in the  $\beta$ -spherulites or the interface between the  $\alpha$ - and  $\beta$ -spherulites, judging from the fact that crystal transition from  $\beta$ - to  $\alpha$ -crystals is not observed in this time domain.

The result of the observation of the drawing behavior through macrobeams suggests that  $\beta$ -crystals disappear when necking occurs to the film and that the  $\beta$ -spherulites participate in the deformation even before the occurrence of necking. However, the beam size of the macrobeam is larger than the spherulite size by two digits, and thus the structural evolution of the  $\beta$ -spherulites, i.e. transformation to oval-shaped hollows could not be observed clearly.

Subsequently, the WAXD-SAXS simultaneous measurement was conducted using a microbeam as the radiation source. The measurement was conducted at the Frontier Soft-material Beamline Consortium (BL03XU) of SPring-8. The above beamline started in 2010 under an industry-university consortium organization for the purpose of promoting basic research on polymer science by using the world's top class radiation source while at the same time strategically using the facilities of industry.<sup>11), 12)</sup> Sumitomo Chemical Co., Ltd. is also participating in the consortium as one of the 19 member companies. Prior to the measurement we attempted to develop a simultaneous measurement/observation tech-

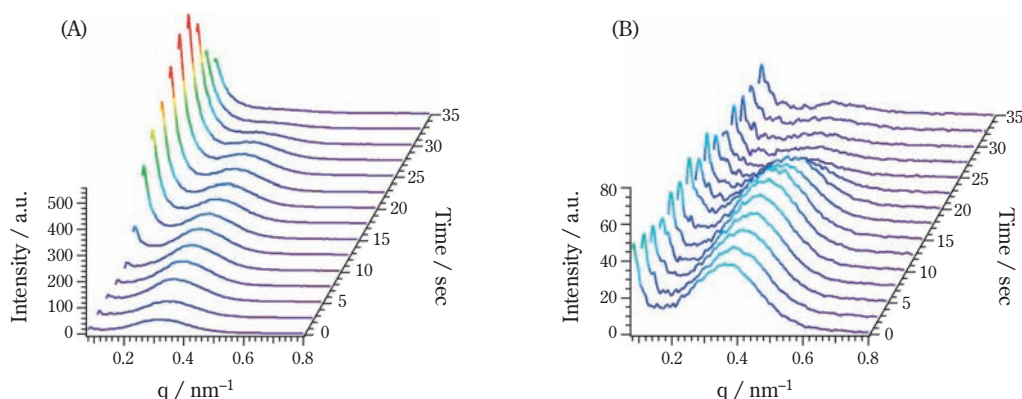


**Fig. 8** Time evolution of circular averaged SAXS profiles observed for (A) film with  $\alpha$  and  $\beta$  spherulites, and (B) film with only  $\alpha$  spherulites during MD drawing

nique for X-ray diffraction, scattering and microscopic observation using BL03XU. **Fig. 9** shows the optical system. As shown in **Fig. 10**, by optimizing the optical microscopic-observation system in the microbeam optical system with a 10  $\mu\text{m}$  pinhole, we had successfully traced the time evolution of the crystalline structure of the local area while simultaneously observing the high-resolution POM image.

**Fig. 11** shows the time evolution of POM images when the film having  $\alpha$ - and  $\beta$ -spherulites is drawn and that of the WAXD and SAXS profiles in a single  $\beta$ -spherulite. For this experiment a film with a thickness

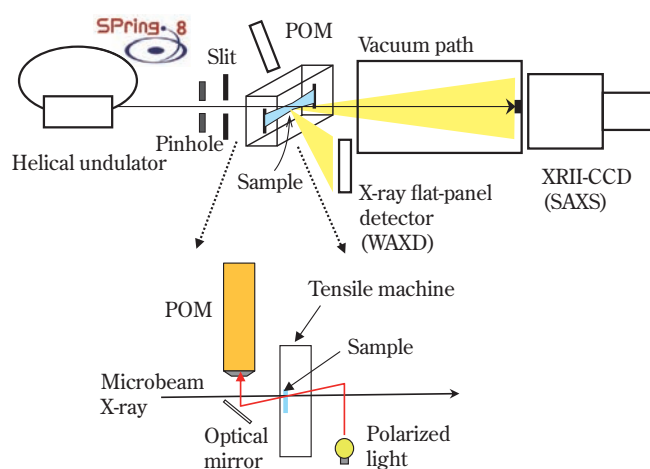


**Fig. 9** Experimental system for microbeam WAXD-SAXS and POM simultaneous measurement

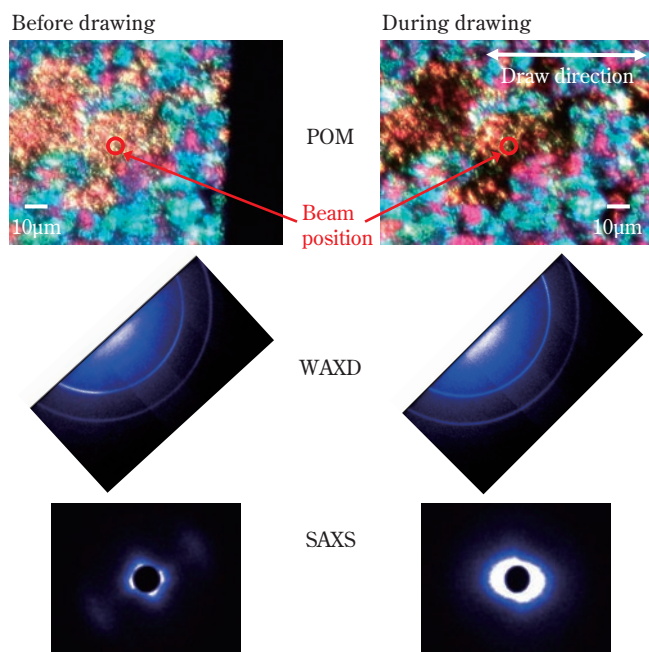


**Fig. 10** Representative POM-WAXD-SAXS data sets during MD drawing

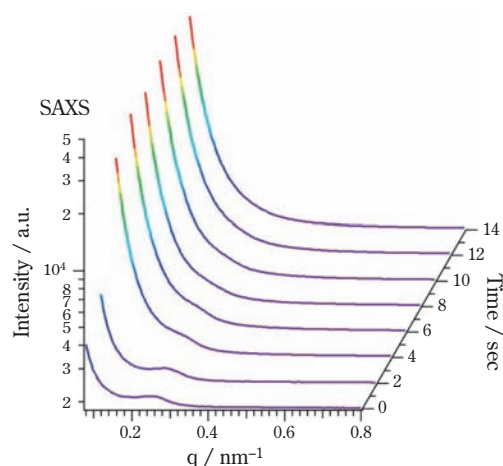
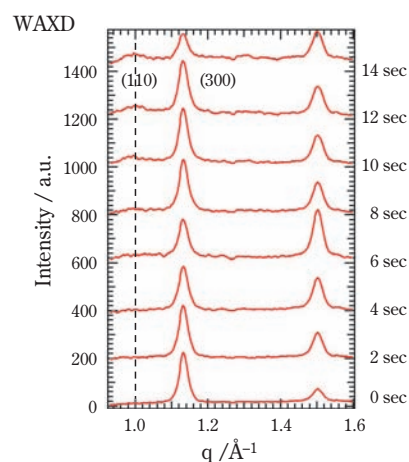
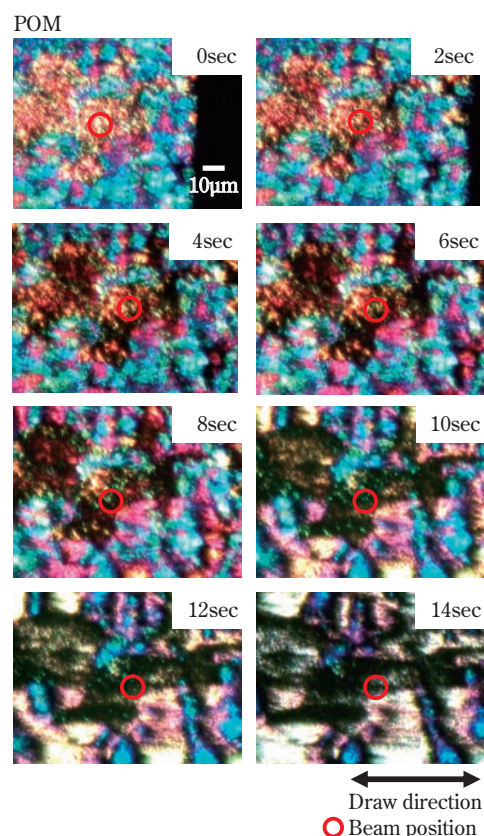


**Fig. 11** Time evolution of POM images and circular averaged WAXD and SAXS profiles in “a”  $\beta$ -spherulite during MD drawing

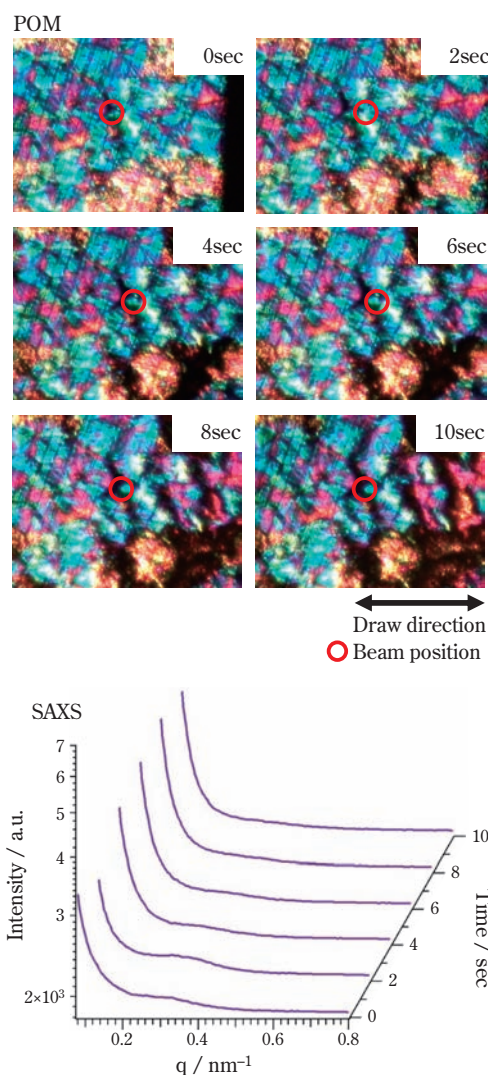


**Fig. 12** Time evolution of POM images and circular averaged SAXS profiles in “an”  $\alpha$ -spherulite during MD drawing

of 30  $\mu\text{m}$  made by cutting off the cross section of the original undrawn sheet with an ultramicrotome was used as a specimen. The drawing temperature was set at 100°C. In the POM images one can observe that the  $\beta$ -spherulites are selectively being deformed and that strong scattering in the lower  $q$  range occurs in SAXS from the early stages of the drawing process. Moreover, the formation of  $\alpha$ -crystals can be seen at around 10 sec. where the morphology of  $\beta$ -spherulite begins to disappear in the POM images. On the other hand, **Fig. 12** suggests that no strong scattering in the lower  $q$  range occurs in the time evolution of the SAXS profile in a single  $\alpha$ -spherulite.

From the result of examination using synchrotron radiation, we were able to obtain useful information about the formation mechanism of surface roughness formed on polypropylene films for capacitors. The

results of the experiment also suggested that the difference in the drawing properties between  $\alpha$ - and  $\beta$ -spherulites plays an important role in the production of oval-shaped hollows. It can be expected that research to clarify the mechanism (e.g., effect of crystal transition from  $\beta$  to  $\alpha$ ) will further progress in the future.

## Observation of the Three-Dimensional (3-D) Morphology of Compounds

### 1. Applications to Organic Fiber Reinforced Polypropylene

As the interest in environmental load reduction grows, the market is hoping for the improvement of the performance and functionalities of materials while reducing the weight of the materials. For electronics products and automobile components, metal and engineering plastics have gradually become replaced by polypropylene materials. For such replacements, it is essential to improve the mechanical properties of polypropylene. In order to achieve this goal, the addition of fiber within polypropylene is one effective technique. Glass fiber-reinforced polypropylene, which has already been put to use, is a typical example. Research and development of polypropylene with biomass such as kenaf and organic fibers have recently been carried out as well. It is also considered that organic fiber-reinforced polypropylene is lighter than glass fiber-reinforced polypropylene, and thus has well-balanced processability and mechanical properties.

Expectations for such polypropylene are high due to its advanced practicability. For the development of this compound, it is important to control the dispersion of the fiber contained in polypropylene. A nondestructive three-dimensional observation technology will therefore be required in order to observe the morphology of the fiber.

An imaging method using X-ray CT (Computed Tomography) is useful as a means to observe the internal structure of the compound with nondestructive micro-scale spatial resolution; therefore it is commonly used in many industrial fields for nondestructive testing of various products. When observing the inside of the compounds using X-ray CT, the measuring method and conditions change depending on the X-ray absorption ability of the substance constituting the material. For example, in a compound composed of polypropylene and organic fiber, both polypropylene and organic fiber have low X-ray absorption, and in this respect the dif-



ference between the two substances is small. It is therefore favorable to measure at high sensitivity in order to observe both polypropylene and organic fiber simultaneously and more precisely. This paper introduces the observation technique using X-ray CT and examples of the observation of the newly developed organic fiber-reinforced polypropylene.<sup>13), 14)</sup>

## 2. Special Features of Organic Fiber Reinforced Polypropylene

The newly developed organic fiber-reinforced polypropylene has been produced through the following procedure: A fiber bundle made of several thousands of high-strength polyester fibers, each of which has a diameter of 30  $\mu\text{m}$ , is impregnated with high-performance polypropylene. The fiber bundle is then cut to the desired length (usually ranging from 5 to 15 mm) and made into pellets. It is possible to mass-produce organic fiber-reinforced polypropylene bodies using a general-purpose injection molding machine as well as related technology.<sup>15)</sup> The organic fiber-reinforced polypropylene body is not only light (the relative weight is 0.99 at a fiber content of 25 wt%, and the relative weight is 1.01 at a fiber content of 30 wt%), but also demonstrates higher impact strength compared to other conventional polypropylene bodies used for instrument panels and bumpers.

Fig. 13 shows the photos taken during high-speed impact testing conducted at a temperature of  $-30^{\circ}\text{C}$ . It can be observed that while the regular instrument panel is completely destroyed, the performance of the organic

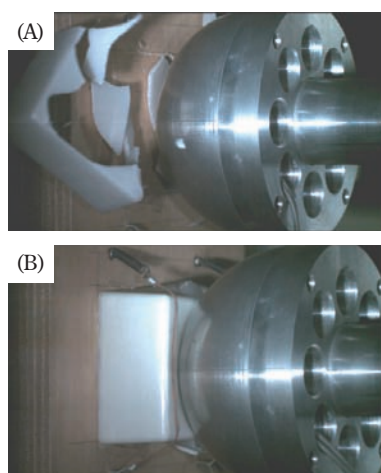


**Fig. 13** Snap shots of high-speed impact testing at  $-30^{\circ}\text{C}$  for instrument panel made from (A) polypropylene compound and (B) fiber-reinforced polypropylene compound

fiber-reinforced polypropylene body shows that although the weldment becomes cracked, the whole body does not become destroyed.

## 3. Observation of the Fiber Dispersion

X-ray CT has been developed based on Radon's image reconstruction theory, whereby a two- or three-dimensional object can be primarily reproduced from an infinite set of projection data. Thus X-ray CT is a technology for reconstructing cross-section images from a projection by taking the X-ray photos of an object from various angles. When an electromagnetic wave such as an X-ray passes through a substance, changes in intensity due to absorption and in the phase of the X-ray occur. Commercially available industrial X-ray CT apparatus converts the level of this X-ray intensity change (absorption contrast), as caused by absorption, into images.

Fig. 14 indicates a schematic illustration of an industrial X-ray CT apparatus. It has a structure in which the X-ray source and detector are fixed, and the specimen is rotated by a revolving stage. The mainstream X-ray source is a cone beam which is radiated from a micro-focus point of the X-ray of less than several microns. Also, the mainstream X-ray detectors are a flat panel X-ray CCD detector and another with a beryllium window image intensifier. The X-ray energy to be generated varies depending on the tube voltage (strictly speaking, it also depends on the tube current) with a range from several tens to several hundreds of kV when using an industrial X-ray CT apparatus. The higher the tube voltage is, the greater the X-ray energy will be, thus allowing the specimen to transmit more easily. Furthermore, if the X-ray energy reaching the X-ray detector is smaller than the detector's minimum limit of detection, it will be more difficult to obtain transmission images. Therefore, it is a general practice that high X-ray energy is

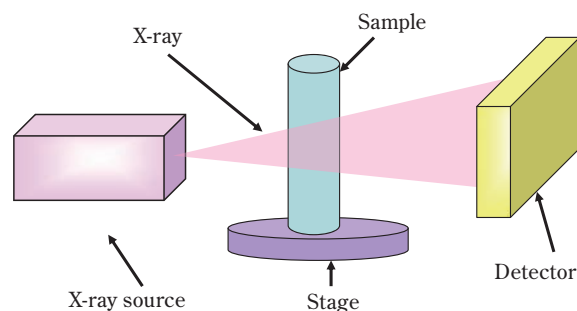


**Fig. 14** Schematic illustration of X-ray CT apparatus



used when taking X-ray absorption images of a substance with higher density such as metal or a thick specimen, while low X-ray energy is used when taking X-ray absorption images of a substance with lower density or a thin specimen.

**Fig. 15** shows an example of X-ray CT image of an organic fiber-reinforced polypropylene body (with a fiber content of 30 wt%) made by injection molding. In this figure, the bright area indicates the fiber while the dark area indicates the resin. Additionally, when observing organic fiber-reinforced polypropylene, it is effective to reduce the X-ray energy as low as possible. For this reason the observation was carried out under the lower limit of the apparatus (20 kV). Through a comparison with glass fiber polypropylene, it has been revealed that in organic fiber-reinforced polypropylene, the fibers are distorted, evenly dispersed and complicatedly entangled with each other. It can therefore be assumed that the impact resistance unique to organic fiber-reinforced polypropylene is derived from this fiber entanglement.

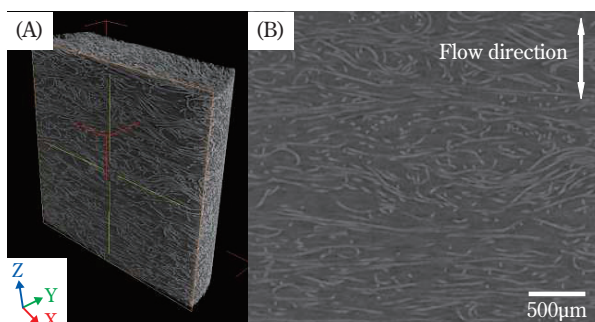


**Fig. 15** Representative X-ray CT images of fiber-reinforced polypropylene compound: (A) 3D image and (B) cross section of X-Z plane

We have successfully demonstrated, in the course of this study, that the X-ray CT can be a useful method for the nondestructive internal observation of compounds consisting of light-elements such as organic fiber-reinforced polypropylenes in addition to the conventional glass fiber-reinforced polypropylenes. Moreover, in recent years the industrial application of imaging technique using synchrotron radiation X-ray as the beam source—by which the shift of the phase of X-ray (phase contrast) is measured and converted into images—has become increasingly popular. This X-ray imaging is extremely sensitive as compared to the absorption contrast method, and there is a

report on the case in which all the components of the compound composed of light and medium-heavy elements such as signal cables were simultaneously and very delicately visualized in a short period of time.<sup>16)</sup> One can therefore say that expectations will continue to grow with respect to this observation method.

#### 4. Observation of Bodies Obtained by Injection Molding After Tensile Testing

It is effective for the investigation of the mechanism of mechanical properties to observe the bodies obtained by injection molding after tensile testing. **Fig. 16** (A) and (B) show the X-ray CT images of bodies obtained by injection molding after tensile testing. The body (A) has a fiber diameter of 33  $\mu\text{m}$ , and the body (B) has a fiber diameter of 18  $\mu\text{m}$ . The fiber content is 25 wt% for both bodies. As well, the plane impact strengths of (A) and (B) are 19.0 J and 16.5 J, respectively.

In the YZ cross-sectional images (A) in **Fig. 16**, it can be observed that there are horizontal cracks in the resin region indicated by a black color. Additionally, in the resin region in the XY cross-sectional image it can be recognized that numerous black holes are left behind after fibers have fallen out. However, in the XZ cross-sectional images (B) in **Fig. 16** no horizontal cracking can be seen and only a small number of holes are left behind after fibers have fallen out. When the fiber diameter is small, the strength of each fiber is insufficient, thus causing fiber breaking during tensile testing. Conversely, when the fiber diameter is large, fiber fall-out occurs more often than fiber breaking during tensile testing. From these observations it is obvious that the destruction behavior of compounds varies according to the fiber diameter.

**Fig. 17** shows X-ray CT images of the area 20 mm away from the fracture front of the body obtained by injection molding. Even in the area 20 mm below the actual fracture front, cracks indicated by a black color can be seen in the direction crossing the tensile test specimen. Furthermore, from the enlarged view of those cracks one can see that they are derived from the fibers oriented toward the direction perpendicular to the paper surface. This suggests that the cracks are caused by the separation of resin and fibers that are oriented perpendicular to the tensile direction when their interface can no longer bear the stress due to insufficient interfacial adhesions of fiber and resin. From this result it is obvious that in order to further improve the impact resistance of organic fiber-reinforced polypropy-

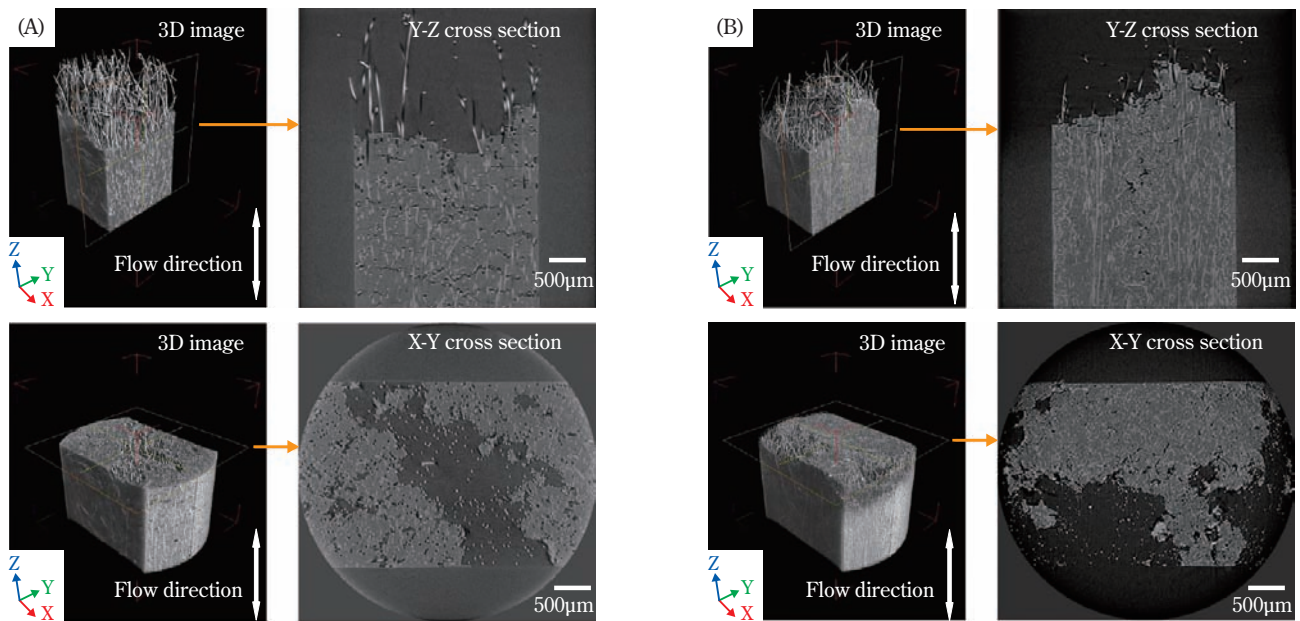


**Fig. 16** (A) Representative X-ray CT images of fiber-reinforced polypropylene compound (fiber diameter 33μm) after tensile testing  
(B) Representative X-ray CT images of fiber-reinforced polypropylene compound (fiber diameter 18μm) after tensile testing

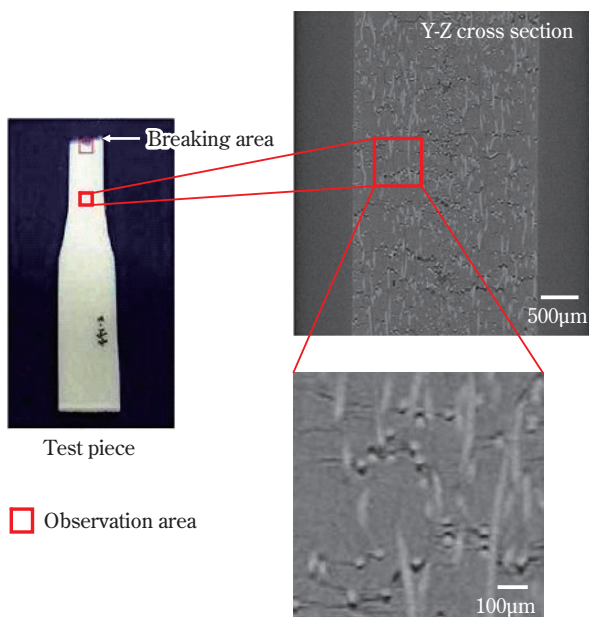


**Fig. 17** Representative X-ray CT images of area in 20mm apart from fracture front of fiber-reinforced polypropylene compound (fiber diameter 33μm) after tensile testing

lene, it is effective to control the fiber orientation and reinforce the interface between fiber and resin.

## 5. Effects of Interfacial Reinforcement

In organic fiber-reinforced polypropylene the plane impact strength can be further improved by reinforcing

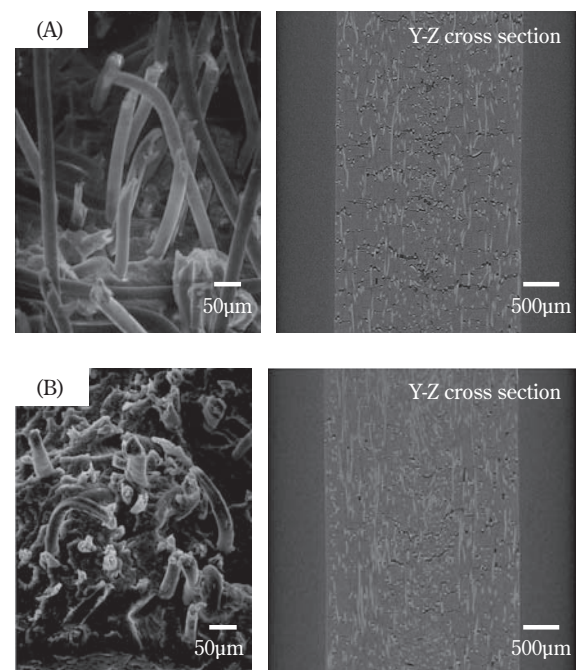


**Fig. 18** Representative SEM images on fracture front (left) and X-ray CT images of area in 20mm apart from fracture front (right) after Izod testing: (A) PP/fiber without interfacial reinforcement and (B) PP/fiber with interfacial reinforcement

the interface between fiber and resin.<sup>17), 18)</sup> **Fig. 18** (A) and (B) show SEM images of the Izod test fracture front and X-ray CT images of the area 20 mm below the

fracture front of the tensile test specimen before and after the interfacial reinforcement. In **Fig. 18 (A)**, which shows images of the compound without reinforcement, no resin adhesion can be confirmed in the SEM image and cracks can be observed in the X-ray CT image.

Conversely, in **Fig. 18 (B)**, which shows images of the compound with reinforcement after the application of an appropriate modifier and a fiber-surface preparation agent to the interface, resin adhesion can be seen in the SEM image and a reduction of cracking can be observed in the X-ray CT image.

## Conclusion

This paper, titled “Application of Material Characterization to Research & Development of Polypropylenes,” has mainly described the analysis of the drawing behavior of films using X-rays and optical techniques such as synchrotron radiation, as well as 3-D morphology observation of compounds using X-ray CT. The technique with which to simultaneously observe the hierarchical structure of polypropylene through the combination of multiple methods provides extremely useful information for understanding the correlation between the structure and properties. Furthermore, it can be expected that nondestructive 3-D observation techniques for compounds will become increasingly important as material design becomes more complex and diverse.

Structural analysis techniques have progressed tremendously in recent years. Of those techniques, various ones (including X-ray free electron laser which is a next-generation synchrotron radiation source and a cutting-edge microscopic observation technique for the observation of the micro world) can now be put to practical use. We have great expectations for further technological innovations with those analysis techniques.

Lastly, part of this study was conducted by using the Frontier Soft-material Beamline Consortium of SPring-8 and the approval of the Photon Factory Proposal Advisory Committee (issue number: 2010G540). We wish to express our deep appreciation to Professor Yoshiyuki Amemiya and Assistant Professor Yuya Shinohara of the Graduate School of Frontier Sciences, the University of Tokyo, who instructed us during this study. We also sincerely appreciate Dr. Hiroyasu Masunaga, Dr. Hiroki Ogawa and Dr. Takumi Takano of the Japan Synchrotron Radiation Research Institute,

who gave us support during the measurements conducted at SPring-8.

## References

- 1) M. Fujiyama, Firumu Seimaku Enshin No Saitekika To Toraburu Taisaku [Optimization and Troubleshooting of Film Drawing Process, Technical Information Institute, 2007, p. 237.
- 2) H. Awaya, Koubunshi Sozai No Henkou Kenbikyoku Nyuumon [Introductory Book of Polarized Optical Microscope for Polymers], AGNE Gijutsu Center, 2001, p. 121.
- 3) E. P. Moore Jr, Pori Puropiren Hando Bukku [Polypropylene Handbook], Kogyo Chosakai Publishing Co., Ltd., 1998, p. 159.
- 4) T. Sakurai, Y. Nozue, T. Kasahara and N. Yamaguchi, SUMITOMO KAGAKU, **2007-II**, 14 (2007).
- 5) T. Sakurai, Y. Shinohara, Seikei Kakou [Seikei-Kakou], **20** (7), 419 (2008).
- 6) T. Sakurai, T. Kasahara and N. Yamaguchi, Koubunshi Kakou [Polymer Processing], **53** (1), 24 (2004).
- 7) T. Sakurai, Y. Nozue, T. Kasahara, K. Mizunuma, N. Yamaguchi, K. Tashiro and Y. Amemiya, *Polymer*, **46**, 8846 (2005).
- 8) Y. Nozue, Y. Amemiya, Housya Kou [J. Jpn. Sci. for Synchrotron Radiation Research], **19**, 356 (2006).
- 9) Y. Nozue, Y. Shinohara, Y. Ogawa, T. Sakurai, H. Hori, T. Kasahara, N. Yamaguchi, N. Yagi and Y. Amemiya, *Macromolecules*, **40**, 2036 (2007).
- 10) Y. Shinohara, K. Yamazoe, T. Sakurai, S. Kimata, T. Maruyama and Y. Amemiya, *Macromolecules*, **45**, 1398 (2012).
- 11) Y. Sugihara, T. Nakao, K. Sakurai, H. Masunaga, H. Ogawa and T. Takano, Pori Fairu [Polyfile], **47** (562), 21 (2010).
- 12) H. Masunaga, H. Ogawa, T. Takano, S. Sasaki, S. Goto, T. Tanaka, T. Seike, S. Takahashi, K. Takeshita, N. Nariyama, H. Ohashi, T. Ohata, Y. Furukawa, T. Matsushita, Y. Ishizawa, N. Yagi, M. Takata, H. Kitamura, K. Sakurai, K. Tashiro, A. Takahara, Y. Amamiya, K. Horie, M. Takenaka, T. Kanaya, H. Jinnai, H. Okuda, I. Akiba, I. Takahashi, K. Yamamoto, M. Hikosaka, S. Sakurai, Y. Shinohara, A. Okada and Y. Sugihara, *Polymer J.*, **43**, 471 (2011).
- 13) K. Watanabe, T. Sakurai, Pori Fairu [Polyfile], **48** (567), 26 (2011).
- 14) K. Watanabe, Jisedai Pori orefin Sougou Kenkyu [Next Generation Polyolefins], **5**, 97 (2011).



15) Jpn. Kokai Tokkyo Koho 2011-26571.

16) A. Yoneyama, K. Ueda, T. Yamazaki, K. Sumitani, Y. Hirai, T. Takeda, K. Hyodo and K. Hirano, Gensiryoku  
eye [Nuclear Energy eys], **55** (8), 32 (2009).

17) Jpn. Kokai Tokkyo Koho 2012-7152.

18) Jpn. Kokai Tokkyo Koho 2012-7158.

PROFILE



*Takashi SAKURAI*

Sumitomo Chemical Co., Ltd.  
Petrochemicals Research Laboratory  
Research Associate  
Doctor of Engineering



*Kenji WATANABE*

Sumitomo Chemical Co., Ltd.  
Petrochemicals Research Laboratory  
Researcher



*Shizuto YAMAKOSHI*

Sumitomo Chemical Co., Ltd.  
Petrochemicals Research Laboratory  
Researcher



*Naoya UMEGAKI*

Sumitomo Chemical Co., Ltd.  
Petrochemicals Research Laboratory  
Researcher